BOREAL ENVIRONMENT RESEARCH 5: 315–336 ISSN 1239-6095
Helsinki 20 December 2000

Characterization of atmospheric trace gas and aerosol concentrations at forest sites in southern and northern Finland using back trajectories

Markku Kulmala[1)], Üllar Rannik[1)], Liisa Pirjola[1)], Miikka Dal Maso[1)], Janne Karimäki[1)], Ari Asmi[1)], Arto Jäppinen[1)], Veli Karhu[1)], Hannele Korhonen[1)], Suvi-Päivi Malvikko[1)], Arto Puustinen[2)], Jukka Raittila[1)], Sami Romakkaniemi[2)], Tanja Suni[1)], Sari Yli-Koivisto[1)], Jussi Paatero[3)], Pertti Hari[4)] and Timo Vesala[1)]

[1)] *University of Helsinki, Department of Physics, P.O. Box 9, FIN-00014 University of Helsinki, Finland*
[2)] *University of Kuopio, Department of Applied Physics, P.O.Box 1627, FIN-70211 Kuopio, Finland*
[3)] *Finnish Meteorological Institute, Sahaajankatu 20 E, FIN-00810 Helsinki, Finland*
[4)] *University of Helsinki, Department of Forest Ecology, P.O. Box 24, FIN-00014 University of Helsinki, Finland*

Kulmala, M., Rannik, Ü., Pirjola, L., Dal Maso, M., Karimäki, J., Asmi, A., Jäppinen, A., Karhu, V., Korhonen, H., Malvikko, S.-P., Puustinen, A., Raittila, J., Romakkaniemi, S., Suni, T., Yli-Koivisto, S., Paatero, J., Hari, P. & Vesala, T. 2000. Characterization of atmospheric trace gas and aerosol concentrations at forest sites in southern and northern Finland using back trajectories. *Boreal Env. Res.* 5: 315–336. ISSN 1239-6095

The trace gas and aerosol concentrations as well as meteorological data (radiation, temperature, humidity) measured in Hyytiälä and Värriö, southern and northern Finland, respectively, were investigated with air mass analyses. The back trajectories of air masses arriving to the sites on the 925-hPa pressure level were calculated 96 hours backwards in time. Two trajectories per day, arriving at 00 UTC and 12 UTC, were computed. The studied time period covered December 1997 to August 1998, November 1998 to July 1999, and September 1999. The arriving air masses were divided into five sectors according to their origin: I = North–West (Arctic Ocean), II = North–East

(Northern Russia, Kola Peninsula), III = South–East (Southern Russia, St. Petersburg), IV = South–West (Central Europe, Great Britain), and V Local, circulating air masses. The climatology of various properties of air masses originating from different sectors was studied. The analysis showed differences between typically clean (sectors I and II) and polluted (sectors III and IV) air masses. In air masses from sectors III and IV, the NO_x concentrations were high during all seasons, but the O_3 concentrations were high during the spring and summer seasons and low in winter. The highest SO_2 concentrations arrived from sector III. In Värriö also the air from sector II was accompanied with higher SO_2 concentrations and some very high peaks were observed in winter when air masses passed through the industrial area of Kola Peninsula. Nucleation events typically occurred in clean air masses and accumulation mode concentrations were higher in polluted air masses. Although there were some differences between Hyytiälä and Värriö, the overall behaviour was similar at both sites.

Introduction

Aerosol particles and trace gases are ubiquitous in the Earth's atmosphere and contribute significantly to both biogeochemical cycling and to the Earth's radiative flux budget. Intergovernmental Panel on Climate Change gave in their 1995 report (Houghton *et al.* 1996) an estimation of the globally and annually averaged radiative forcing for the direct and indirect contributions of greenhouse gases, for the direct and indirect aerosol effect, and for natural changes in solar output. Since each of these contributions reflects the integrated effects of various anthropogenic and biogenic pathways, a critical task is to describe the content of each contribution and its sources, and to reduce the uncertainties.

A major problem in the analysis of the environmental issues is a lack of combined physico-chemical and biological knowledge. Practical examples of combination of physico-chemical and biological knowledge and possibility to utilize versatile up-to-date instrumentation for continuous long-term field measurements are illustrated at the SMEAR stations (**S**tation for **M**easuring forest **E**cosystem–**A**tmosphere **R**elations). The facility comprises two installations: SMEAR I in Värriö (northern Finland) and SMEAR II in Hyytiälä (southern Finland). The stations are similarly equipped and form a combined facility operating within the boreal Scots pine forest under different climatic conditions.

The formation of new aerosol particles, called a nucleation event, and the subsequent growth of these particles was observed at SMEAR stations in the 1990s (Mäkelä *et al*. 1997, Kulmala *et al*. 1998, Pirjola *et al*. 1998, Mäkelä *et al*. 2000). Although meteorological, chemical and biological factors are known to affect the particle formation (Kulmala *et al*. 2000), the role of each of these factors is yet to be fully understood. The experimental capacity of both SMEAR stations enables us also to analyse trace gas (O_3, NO_x, SO_2) concentrations, the atmosphere–forest gas exchange, and meteorological factors affecting environmental issues (Ahonen *et al*. 1997, Vesala *et al*. 1998). In this paper, we present trace gas and aerosol properties as well as canopy and shoot scale fluxes measured at SMEAR stations as a function of air masses. The air mass analysis was performed using back trajectories. Although back trajectories typically include some uncertainties (*see* Stohl 1998), they have been used in the source analysis (e.g. Virkkula *et al*. 1995, Virkkula *et al*. 1997, Stohl 1996, Wotawa and Kröger 1999) and also in analysing air pollution according to air mass histories (e.g. Beine *et al*. 1996, Solberg *et al*. 1997, Simmonds *et al*. 1997, Avila and Alarcon 1999). Our aim was to find out the characteristics of aerosol concentrations, trace gas concentrations, canopy scale fluxes, and shoot scale fluxes for different air masses in order to reveal links between air masses, particle formation, canopy gas exchange, and chemistry.

Experiments

SMEAR stations

SMEAR I station (67°46´N, 29°35´E, 390 m a.s.l) is situated in a 40-year-old and 7-m-tall Scots pine (*Pinus sylvestris* L.) stand on the top of a hill at the Arctic timberline. It complements the research done at SMEAR II station by operating under different climatic conditions but representing the same boreal vegetation type. The severe arctic conditions cause an additional challenge to the arrangement of measurements. The annual mean temperature in Värriö is around –1.5 °C and south–west is the prevailing wind direction.

SMEAR II station (61°51´N, 24°17´E, 181 m a.s.l) is located in a homogenous Scots pine stand at Hyytiälä Forestry Field Station of the University of Helsinki, 220 km NW from Helsinki. The natural managed stand was established in 1962 by sowing after the area had been treated with prescribed burning and light soil preparation. The stand consists only of 1% of other species besides Scots pine close to the station. The mean height of the trees on the site is 12 m, their mean diameter at the breast height is 13 cm, and the projected leaf area is 3 m^2 (8 m^2 in the case of total area) per unit area of soil. The air quality at the site represents typical background conditions. The annual mean temperature in Hyytiälä is 3 °C.

Practically no local sources of pollutants exist close to the SMEAR I station. However, regularly occurring episodes of heavy sulphur dioxide and aerosol pollution are observed during northeasterly winds, transported from the Kola Peninsula industrial areas (Ahonen *et al*. 1997, Virkkula *et al*. 1997), which are located less than 200 km away from Värriö. The St. Petersburg area and Russia have been determined as being source areas for SO_2, O_3 and fine aerosol particles (Virkkula *et al*. 1995, Beine *et al*. 1996). Also the continental Europe and British Isles are responsible for pollution in Finnish Lapland (Virkkula *et al*. 1995, 1997). The continental Europe is a source of NO_x all over the year, such that the production and depletion of O_3 occurs in summer and winter, respectively (Laurila 1999, Simmonds 1997). These are also the main known source areas for pollution at SMEAR II, with the exception that Kola industrial areas influence less and St. Petersburg and Central and Western Europe more the air quality in Hyytiälä. The local pollution from the station buildings (0.5 km) and the city of Tampere (60 km), both located west-south-west from the station, affect occasionally the air quality at SMEAR II.

More information on the sites as well as details of measurements can be found in Ahonen *et al*. (1997), Hari *et al*. (1994) and Vesala *et al*. (1998), *see also* the SMEAR homepage at http://honeybee.helsinki.fi/HYYTIALA/smear), and the EU funded project BIOFOR (Biogenic aerosol formation in the boreal forest) homepage (http://mist.helsinki.fi/Biofor/index.html).

Back trajectories

The air mass back trajectories needed in this work were calculated with the long-range transport model TRADOS (Pöllänen *et al*. 1997, Valkama and Pöllänen 1996). The model is an air parcel trajectory model of the Lagrangian type. The three-dimensional trajectories and the dispersion parameters are computed by using numerical meteorological forecasts obtained from the Nordic HIRLAM (**H**igh **R**esolution **L**imited-**A**rea **M**odel) weather prediction model which contains 31 vertical levels. The horizontal grid resolution of the HIRLAM version used in this study was 44 × 44 km. Parameters obtained from the HIRLAM database are the surface data (the surface pressure and ground surface temperature, air temperature, relative humidity, surface wind speed, and precipitation) and the pressure level data (ambient air temperature, relative humidity, vector wind, and geopotential height) at seven different constant pressure levels: 1 000, 925, 850, 700, 500, 300, and 100 hPa.

In the present study, air parcel back trajectories arriving at Hyytiälä and Värriö on the 925-hPa pressure level were calculated typically 96 hours (66% of trajectories belonging to classes I to IV, *see* next section for trajectory classes) backwards in time. The trajectories were shorter in time when they left the geographical region of the current version of HIRLAM, approximately the area between (47°N, 103°W), (88°N, 180°E), (62°N, 100°E), (50°N, 55°E), (27°N, 33°E), (35°N, 0°E), (22°N, 43°W), and (37°N, 70°W), i.e. from cen-

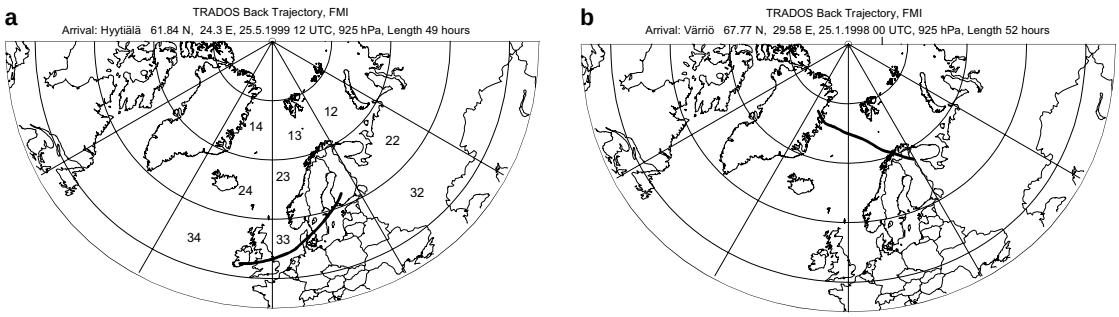

Fig. 1. — a: 49 hours long TRADOS back trajectory arriving at Hyytiälä 25 May.1999 12 UTC on the 925 hPa pressure level; — b: 52 hours long back trajectory arriving at Värriö 25 Jan.1998 00 UTC on the 925 hPa pressure level.

tral Canada to North Pole, central Siberia, Caspian Sea, Egypt, Gibraltar Strait, central Atlantic Ocean, and Eastern USA. The 925-hPa level was chosen because the TRADOS output for the 1000-hPa level is generally less accurate due to topography effects. Two trajectories per day, arriving at 00 UTC and 12 UTC, were computed. The time period covered from 3 Dec. 1997 to 22 Aug. 1998, from 18 Nov. 1998 to 28 Jul. 1999 and from 9 Sep. 1999 to 22 Sep. 1999.

Trajectory classification

The trajectories were plotted on maps and which their classification established (*see* Fig. 1). The area was divided into squares 30° times 10° in longitudional and latitudional directions. All the grid squares were numbered and all the squares that the trajectory passed through were tracked. If the trajectory passed the areas of a special interest (Kola Peninsula), this was also marked. According to this analysis, trajectories were divided into five main classes corresponding to four main directions (Table 1). If the trajectory did not belong clearly to classes I to IV or it was circulating around Finland, it was not considered in the following analysis (class V). The back trajectories coming from sector IV to Hyytiälä and from sector I to Värriö are presented in Fig 1a and b, respectively. The definition of these four areas was based on the large-scale concentration data of

Table 1. Sectors used in trajectory classification.

Sector	Code	Comments[1)]
The Arctic Ocean, N–W	I	Trajectories originating from squares 12, 13, 14, or 24, and not passing over pollution sources or square 22
Russia northeast of Finland, N–E	II	Trajectories that passed square 22 before arriving to the measurement site
Kola Peninsula (Värriö only)	IIb	Trajectories passing Kola Peninsula
Russia southeast of Finland, S–E	III	Trajectories for which the last or second to last square passed through was 32
Central Europe and Great Britain, S–W	IV	Trajectories for which the last square was 33 or 34
Not classified	V	Not belonging to I to IV

[1)] Routes for different classes, i.e. the combinations of squares corresponding to a certain class, were determined by plotting all the trajectories and choosing the appropriate class for all the combinations of squares the trajectories passed.

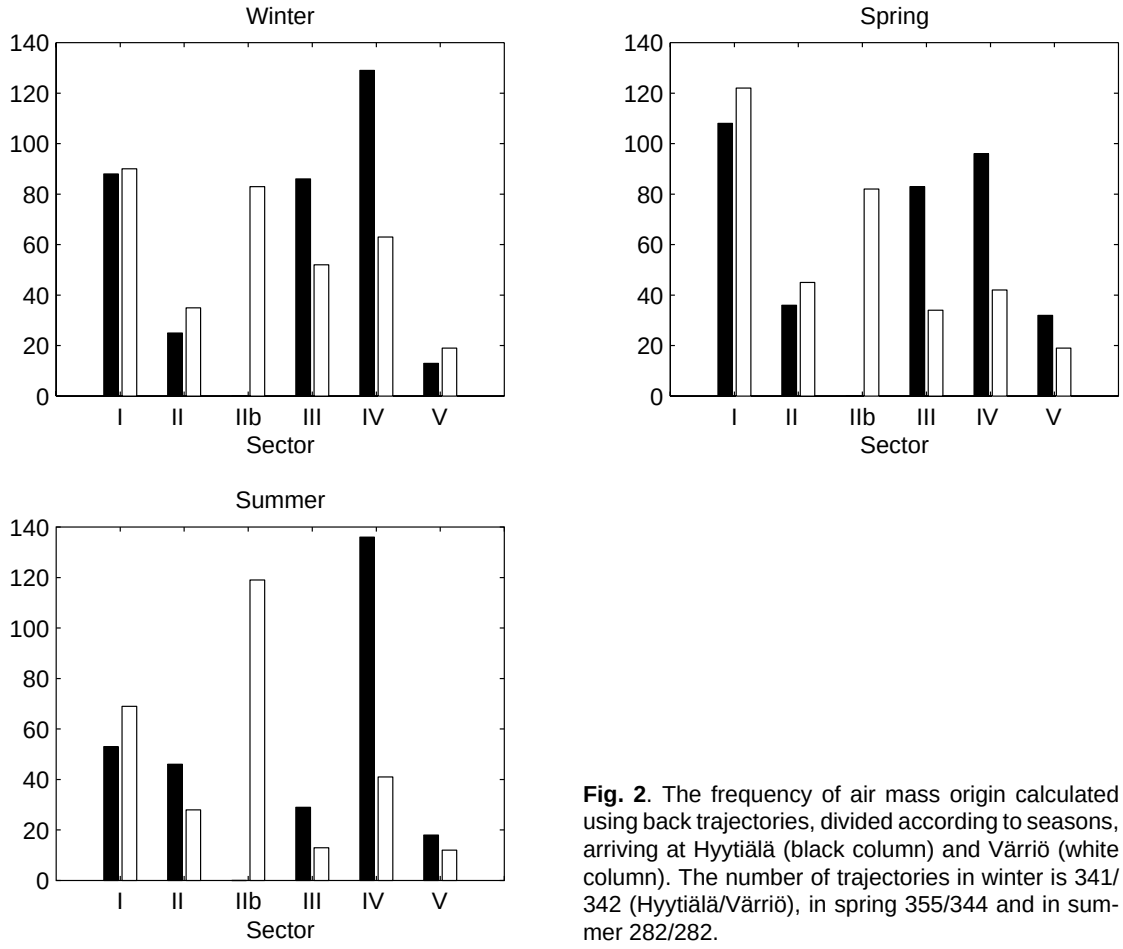

Fig. 2. The frequency of air mass origin calculated using back trajectories, divided according to seasons, arriving at Hyytiälä (black column) and Värriö (white column). The number of trajectories in winter is 341/342 (Hyytiälä/Värriö), in spring 355/344 and in summer 282/282.

various air pollutants (Tarrasón *et al*. 1998, Hjellbrekke 1999). According to Kahl *et al*. (1989), only large geographical domains can be identified with trajectory statistics.

The number of trajectories coming from each sector during different seasons to Hyytiälä and Värriö are presented in Fig. 2. The seasons were defined according to months as follows: winter (December, January, February), spring (March, April, May) and summer (June, July, August). Since the trajectories were available only for a short period in autumn, this season was not analysed separately. The air masses arriving from sector IV dominated in Hyytiälä (more than 350 during the whole period). However, in spring the sector I was dominating. In case of Värriö, the arriving air masses originated equally frequently from sectors I and II + IIb. The extra sector IIb directly from Kola Peninsula industrial areas is important for the air quality in Värriö and was analysed separately for gas and particle concentrations. Corresponding observations were not then included in class II results. The trajectory sectors I and II (+IIb for Värriö) were much more dominating for Värriö than for Hyytiälä. This is in accordance with long-term wind direction statistics (Tammelin 1991) as well as with trajectory flow climatology in northern Finland reported by Rummukainen *et al*. (1996).

Results and discussion

In the following the meteorological parameters (radiation, temperature, humidity), gas (CO_2, H_2O, O_3, NO_x, SO_2) and aerosol concentrations, the micrometeorological fluxes of momentum, heat CO_2, H_2O and aerosol particles, and shoot scale

gas exchange were analysed according to the origin of the arriving air masses and seasons. Table 2 summarises the analysed parameters and observation levels. The observed range of variation was described by percentile statistics, which are not very sensitive to possible erroneous results in observations. In Tables 3 and 4, a summary of statistics is presented. Before statistical analysis, to suppress short turbulence-time-scale variations in observations, the averages of the measured quantities were calculated around the arrival time of trajectories over forty minutes (aerosol particle concentrations) to hourly (all other quantities) period.

Meteorology

Wind direction

Measurements of wind direction in Hyytiälä and Värriö were compared with the directions of arriving trajectories. The wind direction was measured at 50 meters height in Hyytiälä and at 10 meters height in Värriö. The trajectories arriving at Hyytiälä and Värriö on the 925-hPa pressure level were used. The corresponding height depends on surface pressure and is about 600 meters when surface pressure is 1000 hPa.

In the boundary layer the wind direction is not generally constant with height. Frictional forces, temperature advection, and topography affect the wind direction. Because boundary layer friction decreases with height, wind direction tends to turn clockwise with increasing height in the northern hemisphere (Holton, 1992). Cold and warm air advection cause counterclockwise and clockwise turning of wind direction with height, respectively. At Hyytiälä the wind direction was generally by 20–30 degrees more at 925-hPa pressure level than at 50 meters height. This difference was quite independent of the wind direction. At Värriö, however, the respective difference was dependent strongly on the wind direction. This implies the effect of local topography on the wind direction close to the surface.

Temperature

In winter and in spring, the lower temperatures in Hyytiälä corresponded to northeast and southeast air masses. This did not apply to the spring season in Värriö (temperatures for winter were not available). In summer, the air coming from southeast and southwest was generally warmer, and the

Table 2. List of parameters and observation levels at the SMEAR stations, relevant to current study.

Parameter	Measurement level, SMEAR I	Measurement level, SMEAR II
Wind direction	10 m	50 m
Temperature	15 m	67 m
Global radiation	15 m	15 m
UVA and UVB	15 m	15 m
RH		67 m
O_3	15 m	67 m
NO_x	15 m	67 m
SO_2	15 m	67 m
H_2O		67 m
CO_2		67 m
Particle concentration	15 m	2 m
Size distribution (3–500 nm)		2 m
Exchange CO_2, H_2O, NO_x and O_3 by shoots	Canopy top	Canopy top
Turbulent fluxes of momentum, heat, CO_2, H_2O and aerosol particles (bigger than 10 nm in diameter) by eddy covariance		23.3 m and 46.0 m

Table 3. Percentile statistics for parameters measured at Hyytiälä corresponding to trajectory arrival classes during different seasons.

Percentile	Winter				Spring				Summer			
	I	II	III	IV	I	II	III	IV	I	II	III	IV
Temperature (°C) at 12 UTC												
10	–11	–18	–18	–6.2	–3.8	–5.9	–4.7	1.0	13.2	11.0	14.7	13.5
25	–6.3	–15	–14	–2.8	0.5	–4.3	–1.6	2.5	14.2	14.7	16.4	15.4
50	–2.7	–9.7	–7.1	0.0	5.8	4.0	3.1	8.0	16.7	16.7	19.4	18.4
75	–0.2	–6.7	–3.9	1.6	11.0	8.5	6.8	12.0	18.4	19.3	26.0	21.2
90	1.4	–5.2	–0.1	3.0	15.8	9.8	15.3	14.5	21.1	21.4	27.2	24.0
Glob. rad. (Wm^{-2}) at 12 UTC												
10	6	10	4	3	172	135	53	58	152	131	75	121
25	11	36	8	4	261	243	131	128	269	154	199	177
50	24	40	12	8	414	396	291	293	491	226	353	386
75	51	127	41	25	517	569	423	410	611	362	445	549
90	105	238	75	78	588	627	546	546	730	449	663	719
O_3 (ppb) at 00 and 12 UTC												
10	21.8	23.7	12.3	12.2	35.4	26.6	32.0	31.4	22.5	16.9	22.9	25.3
25	27.0	26.1	20.1	17.4	37.8	31.5	38.4	35.4	26.5	23.2	27.6	32.4
50	29.8	30.0	24.2	23.2	41.3	39.6	44.9	42.3	29.3	30.9	36.4	36.9
75	35.0	35.3	27.7	29.0	45.2	41.1	52.1	49.3	34.8	35.3	45.9	43.8
90	37.8	36.5	33.3	33.5	47.6	41.8	57.9	53.9	41.4	39.9	52.2	50.3
NO_x (ppb) at 00 and 12 UTC												
10	0.9	1.1	1.4	1.3	0.7	0.5	1.5	1.3	0.3	0.5	0.8	0.8
25	1.1	1.4	1.9	2.0	0.9	0.7	1.9	1.8	0.5	0.7	1.1	1.0
50	1.7	1.6	2.9	2.9	1.2	0.9	2.6	2.7	0.8	0.9	1.4	1.3
75	2.6	2.5	4.4	4.4	1.7	1.7	3.3	4.1	1.1	1.2	1.6	1.6
90	4.0	3.7	6.7	6.9	2.6	2.3	4.7	5.5	1.4	1.4	1.8	2.3
SO_2 (ppb) at 00 and 12 UTC												
10	0.1	0.1	0.5	0.1	0.1	0.1	0.2	0.1	0.1	0.1	0.1	0.1
25	0.1	0.1	0.8	0.1	0.1	0.2	0.6	0.2	0.1	0.1	0.1	0.1
50	0.2	0.7	1.3	0.3	0.2	0.5	1.1	0.4	0.1	0.1	0.2	0.1
75	0.6	1.2	2.6	0.7	0.4	0.7	1.6	0.8	0.2	0.2	0.5	0.2
90	1.1	2.2	4.3	1.5	0.9	1.3	2.1	1.4	0.3	0.3	0.7	0.4
H_2O (gm^{-3}) at 00 and 12 UTC												
10	2.3	1.4	1.4	3.8	2.3	1.9	2.5	4.5	6.8	8.1	9.3	10.8
25	3.3	1.8	1.9	4.9	3.1	2.3	3.0	5.3	8.7	9.8	11.9	11.6
50	4.4	2.5	3.1	6.0	4.5	3.1	4.1	6.9	10.4	11.1	13.9	13.0
75	5.5	3.8	4.1	6.5	5.6	4.1	6.2	8.7	11.8	13.1	16.3	14.3
90	6.2	4.2	5.2	7.1	6.3	6.9	7.7	10.1	12.7	13.9	17.6	16.5
CO_2 (ppm) at 00 and 12 UTC												
10	356.9	359.3	363.7	360.7	355.9	355.2	359.0	360.6	349.6	350.2	349.8	351.5
25	361.9	360.4	365.3	365.1	358.8	357.1	362.0	361.9	353.1	352.9	354.1	355.1
50	364.5	364.1	369.0	369.1	363.1	363.9	369.2	368.5	358.4	356.9	360.1	360.2
75	367.8	367.6	372.0	372.5	367.2	367.9	372.2	371.8	365.9	360.9	365.5	365.7
90	370.0	368.4	375.9	376.1	370.0	369.1	373.9	374.6	369.0	364.3	369.8	370.9
Aerosol number concentr. (cm^{-3}) at 12 UTC												
10	821	399	685	707	1380	429	1390	1240	1340	688	970	1390
25	997	873	1060	1030	2270	995	2080	1620	2070	933	1330	1870
50	1510	1050	1410	1480	3290	1160	3490	2870	3310	2010	2160	2230
75	2030	1590	2030	2160	6090	1710	4650	3910	5000	2850	2610	2960
90	2830	2580	3310	2610	9370	3920	7090	4160	5860	4140	2800	3520

continued

Table 3. Continued.

Percentile	Winter				Spring				Summer			
	I	II	III	IV	I	II	III	IV	I	II	III	IV
Nucleation mode number concentr. (cm^{-3}) at 12 UTC												
10	0	0	0	0	14	0	0	0	0	0	0	0
25	12	33	13	16	199	59	2	0	0	14	0	0
50	105	76	60	85	846	238	49	80	20	54	31	52
75	495	293	108	296	2360	556	431	261	388	130	48	195
90	644	542	281	776	3950	3520	2050	843	452	218	121	613
Aitken mode number concentr. (cm^{-3}) at 12 UTC												
10	347	236	162	168	438	207	24	49	0	227	0	57
25	608	373	364	323	674	376	334	305	207	270	503	600
50	755	634	645	750	1250	533	838	646	895	867	695	942
75	1210	1110	1090	1030	2240	776	1430	1350	1270	1460	954	1220
90	1670	2130	1520	1430	3460	1030	1790	1790	3000	1620	1160	2030
Accumul. mode number concentr. (cm^{-3}) at 12 UTC												
10	46	85	289	185	64	87	136	39	0	95	0	199
25	94	154	368	296	109	169	467	233	74	161	131	387
50	214	267	464	418	284	272	709	540	208	493	509	547
75	347	360	715	706	381	351	1390	1130	458	986	721	978
90	443	429	1110	1030	895	422	3070	2710	650	1200	1470	1700
CO_2 exchange of shoot (g m^{-2} s^{-1}) at 12 UTC												
10									0.12	0.12	0.09	0.05
25									0.16	0.14	0.10	0.12
50									0.19	0.17	0.18	0.15
75									0.20	0.22	0.21	0.21
90									0.22	0.22	0.22	0.23
H_2O exchange of shoot (g m^{-2} s^{-1}) at 12 UTC												
10									1.5	0.0	–0.8	0.0
25									2.3	0.1	1.6	1.8
50									5.2	4.4	8.1	5.7
75									7.9	8.7	10.5	8.7
90									10.0	11.5	11.9	10.6
O_3 exchange of shoot (ng m^{-2} s^{-1}) at 12 UTC												
10									49.1	29.0	42.4	49.4
25									57.1	57.1	51.9	58.8
50									64.0	73.8	78.3	75.2
75									79.0	85.7	85.4	84.8
90									86.9	97.8	100	92.8
NO_x exchange of shoot (ng m^{-2} s^{-1}) at 12 UTC												
10									2.1	–3.3	0.1	–0.6
25									3.4	–0.8	0.2	1.2
50									5.6	3.7	6.7	12.1
75									9.8	7.2	15.0	16.2
90									15.8	8.8	17.5	18.5
Aerosol particle number flux (10^6 $m^{-2}s^{-1}$) at 12 UTC												
10					–61	–37	–7.2	–14	–5.1	–4.7	–25	–6.6
25					–29	–1.4	–4.8	–6.9	–5.1	–1.5	–9.6	–2.0
50					–9.5	–0.8	–1.3	–3.7	–2.0	–0.4	–1.6	–1.0
75					–4.3	0.1	1.5	–1.0	–1.0	2.4	–0.0	3.6
90					2.5	6.9	9.5	5.0	2.4	3.6	0.2	10.1

Table 4. Percentile statistics for parameters measured at Värriö corresponding to trajectory arrival classes during different seasons.

Percentile	Winter				Spring				Summer			
	I	II/IIb	III	IV	I	II/IIb	III	IV	I	II/IIb	III	IV
Temperature (°C) at 12 UTC												
10					0.4	–0.5	–0.6	–0.7	7.2	3.9	12.3	11.0
25					1.2	0.1	1.4	–0.1	9.6	7.8	12.9	13.4
50					3.3	1.7	3.1	3.2	12.2	11.9	16.9	16.5
75					6.3	4.2	6.8	5.6	15.8	16.2	19.5	20.2
90					9.5	7.5	13.0	7.7	20.1	19.0	24.8	23.9
Glob. Rad. (Wm^{-2}) at 12 UTC												
10	0	0	0	0	147	134	60	93	176	112	32	116
25	0	1	0	0	263	186	108	104	255	154	94	148
50	4	13	1	0	392	294	204	239	376	295	214	247
75	13	54	38	1	487	411	296	421	536	563	567	602
90	74	161	70	115	559	531	409	527	698	668	642	672
O_3 (ppb) at 00 and 12 UTC												
10	33.1	28.6	18.7	22.9	32.7	25.7	37.1	38.5	21.3	21.2	19.2	24.3
		27.2				23.6				21.3		
25	35.8	31.5	23.8	25.4	38.4	29.5	39.4	42.4	24.1	24.7	24.7	27.9
		32.2				31.4				24.5		
50	39.5	35.9	29.8	29.6	42.3	37.2	43.1	44.7	29.8	28.4	27.5	37.8
		36.2				39.4				29.1		
75	42.0	40.9	37.0	38.0	45.7	43.6	50.4	47.1	34.0	30.2	35.9	44.7
		39.6				41.8				30.6		
90	43.5	42.2	40.2	40.6	48.0	49.1	52.6	53.4	35.7	33.4	38.1	50.8
		43.9				43.9				37.1		
NO_x (ppb) at 00 and 12 UTC												
10	0.0	0.0	0.3	0.1	0.0	0.0	0.8	0.4	0.0	0.0	0.0	0.0
		0.1				0.0				0.0		
25	0.1	0.2	0.7	0.4	0.1	0.1	0.9	0.5	0.0	0.0	0.1	0.1
		0.2				0.2				0.0		
50	0.2	0.4	0.9	0.7	0.2	0.3	1.2	0.8	0.0	0.0	0.2	0.2
		0.4				0.3				0.1		
75	0.3	0.6	1.2	1.0	0.3	0.6	1.5	1.1	0.1	0.1	0.4	0.3
		0.9				0.5				0.3		
90	0.6	0.8	1.7	1.3	0.5	0.9	1.9	1.8	0.2	0.2	0.4	0.4
		1.5				1.0				0.4		
SO_2 (ppb) at 00 and 12 UTC												
10	0.0	0.0	0.8	0.1	0.0	0.0	0.2	0.0	0.0	0.0	0.0	0.0
		0.3				0.0				0.1		
25	0.0	0.5	1.6	0.1	0.1	0.1	0.6	0.1	0.0	0.1	0.1	0.1
		1.0				0.2				0.2		
50	0.1	1.4	2.0	0.3	0.2	1.0	0.9	0.3	0.1	0.3	0.1	0.2
		2.6				0.5				0.4		
75	0.5	2.7	3.2	0.5	0.3	1.5	1.6	0.5	0.2	0.8	0.2	0.3
		5.8				1.4				0.7		
90	1.3	4.3	4.2	0.8	0.8	3.1	3.0	1.9	0.4	1.2	0.2	0.4
		11.3				3.2				1.5		

continued

Table 4. Continued.

Percentile	Winter				Spring				Summer			
	I	II/IIb	III	IV	I	II/IIb	III	IV	I	II/IIb	III	IV
Aerosol number concentr. (cm^{-3}) at 12 UTC												
10	813	382 399	882	707	1020	429 555	1430	2630	933	1200 935	1190	1410
25	949	524 873	1070	1060	2130	996 2070	1430	2630	1790	1200 1390	1190	2020
50	1510	1220 1520	1430	1480	2930	1660 3670	3270	3890	2670	2020 2240	1470	2250
75	2040	1540 2350	1640	1710	5410	2300 3930	3740	3960	3350	2020 3130	1740	3360
90	2470	2290 3000	1970	1920	7810	2900 6630	4450	4650	5180	2500 4140	1740	3520

northern air masses brought with them lower temperatures.

In summer, the median temperature in Hyytiälä varied between 15 and 20 °C at daytime. At night, the temperature was approximately 5 °C lower. In winter, there was more variations in the data, the median was between 0 and –10 °C at day and at night. In Värriö, the median varied between 12 and 17 °C in summer at day and was again lower at night.

Radiation

The global radiation statistics were evaluated for 12 UTC (Fig. 3). The lowest radiation fluxes during all seasons corresponded to trajectories arriving from southwest (III) and southeast (IV) sectors. This reflects the higher cloudiness associated with these air masses. An exception was the summer season in Hyytiälä, when the lowest radiation values were measured during the air masses of northeast origin (sector II). However, in winter this was the direction which gave the highest global radiation values, in Hyytiälä and Värriö 90th percentiles were about 250 and 160 W m^{-2}, as compared with about 100 W m^{-2} corresponding to other sectors. The contrast between these winter and summer radiation values was accompanied by a similar contrast in surface pressure values, which indicates that prevailingly high and low pressure weather systems corresponded to air masses arriving from sector II in winter and summer, respectively. The seasonal migration of weather systems has to be responsible for this. In spring, which is the season of frequent nucleation events as will be seen later, the highest radiation corresponded to northern air masses (sectors I and II).

The UV-A and UV-B radiation statistics behaved similarly to global radiation (not shown). The median of UV-A radiation in summer in Hyytiälä was 25–35 W m^{-2} and in Värriö 15–25 W m^{-2}. In both cases, UV-A radiation intensity in winter was only few watts per square meter. The median of UV-B radiation data in Hyytiälä in summer was 1–1.5 W m^{-2} and in Värriö 0.6–1.1 W m^{-2}. In winter it was less than 0.05 W m^{-2}.

Relative humidity

Relative humidity was measured only in Hyytiälä. In spring and in summer, the median of RH was 50%–70% at daytime, and higher at night. In winter, it was nearly 100%, and the variation of the relative humidity was much smaller than during other seasons. This was due to the low saturation vapour pressure. Back trajectory direction did not have a clear connection to relative humidity, except at daytime in spring and in summer the humidity was higher during southwest winds (sector IV).

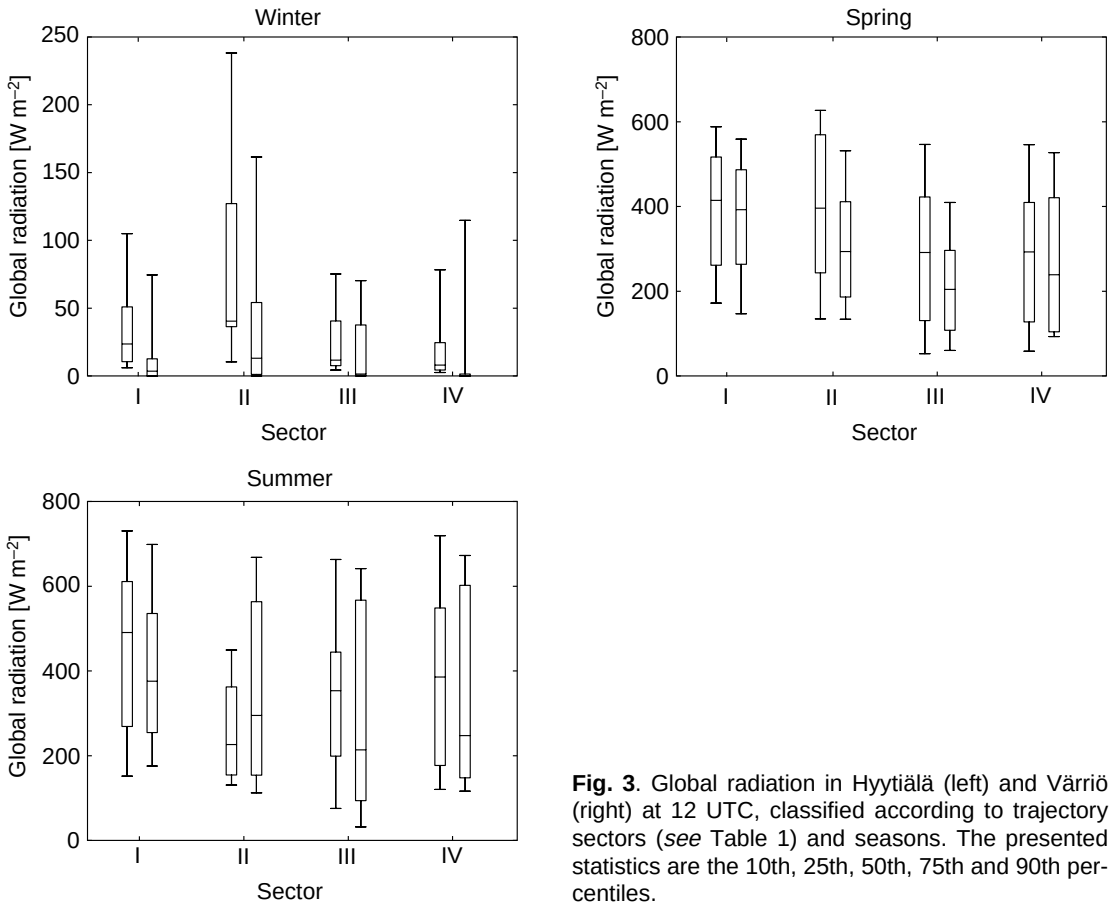

Fig. 3. Global radiation in Hyytiälä (left) and Värriö (right) at 12 UTC, classified according to trajectory sectors (*see* Table 1) and seasons. The presented statistics are the 10th, 25th, 50th, 75th and 90th percentiles.

Gases

The O_3, NO_x and SO_2 concentrations discussed in this section were measured at both the sites. The water and carbon dioxide concentrations were analysed only for Hyytiälä measurements.

Ozone

A seasonal cycle in ozone concentrations was observed. At both the sites the highest ozone concentrations were measured in spring and the lowest in winter (Fig. 4). For example, the seasonal medians in Hyytiälä were 27.2 ppb (winter), 44.1 ppb (spring) and 34.6 ppb (summer). Scheel *et al*. (1997) reported similar behaviour in seasonal differences of O_3: the average concentration in Uto Island (59.8°N, 21.4°E, 7 m a.s.l) was 27.0 ppb in winter and 40.8 ppb in summer over the period 1989 to 1993.

In winter, the higher O_3 concentrations both in Hyytiälä and Värriö corresponded to trajectories from sectors I (the Arctic Ocean) and II (north-west Russia). On the contrary, in spring there were observations of higher O_3 concentrations from sectors III (south-west Russia, including St. Petersburg's area) and IV (Central Europe), even though the distributions were rather wide. Also Beine *et al*. (1996) observed higher ozone concentrations at Ny-Ålesund Zeppelin mountain station (78°55´N, 11°53´E, 474 m a.s.l) in air masses from Russia and Western Europe during the spring season in 1994. This is consistent with the results of Laurila (1999) and Simmonds (1997) on the behaviour of continental Europe as a source and sink of O_3 in summer and winter, respectively. In winter the polluted air masses (sectors III and IV)

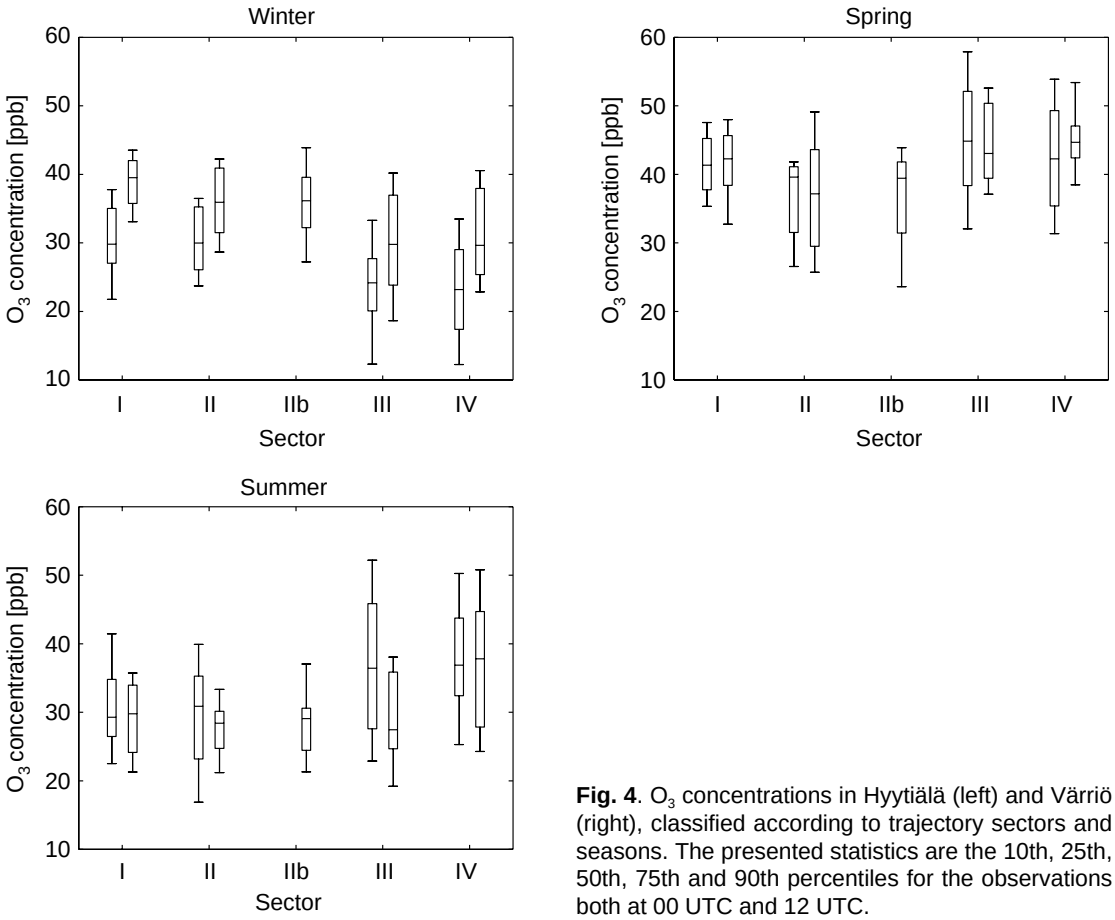

Fig. 4. O_3 concentrations in Hyytiälä (left) and Värriö (right), classified according to trajectory sectors and seasons. The presented statistics are the 10th, 25th, 50th, 75th and 90th percentiles for the observations both at 00 UTC and 12 UTC.

act as a sink for O_3, and in spring when the photochemical reactions start to play an important role, the polluted air masses behave also as a source for O_3 (for chemistry see Seinfeld and Pandis 1998, Finlayson-Pitts and Pitts 2000). Thus the biggest seasonal variation between the winter and spring O_3 concentrations was from sectors III and IV.

In summer, ozone concentrations were lower than in spring, being highest from sector IV (Central Europe) in Värriö and also from sector III (south-west Russia) in Hyytiälä. In summer, when the photochemical radical production is not a limiting factor as in winter, ozone production is more sensitive to NO_x concentrations (Kleinman 1991). The NO_x concentrations were lowest in summer (Fig. 5). Also the dry deposition velocity onto the vegetation is higher in summer due to stomatal activity.

Only a small difference between the nighttime and daytime values of ozone were observed during all seasons in Värriö, but in Hyytiälä the diurnal cycle was clearly seen, especially in summer. At night the concentration decreases because of deposition and limited transport from above due to stable stratification, but at day O_3 is transported from above due to intensive mixing and there is additional photochemical production of O_3 (*see also* e.g., Lopez *et al*. 1993). The difference between Hyytiälä and Värriö can be explained by the same mechanisms: larger deposition due to vegetation characteristics and more photochemical production due to higher NO_x concentrations in Hyytiälä.

Nitrogen oxides

Maximum NO_x concentrations were observed in winter and spring at both the sites (Fig. 5). The lowest seasonal NO_x concentrations were meas-

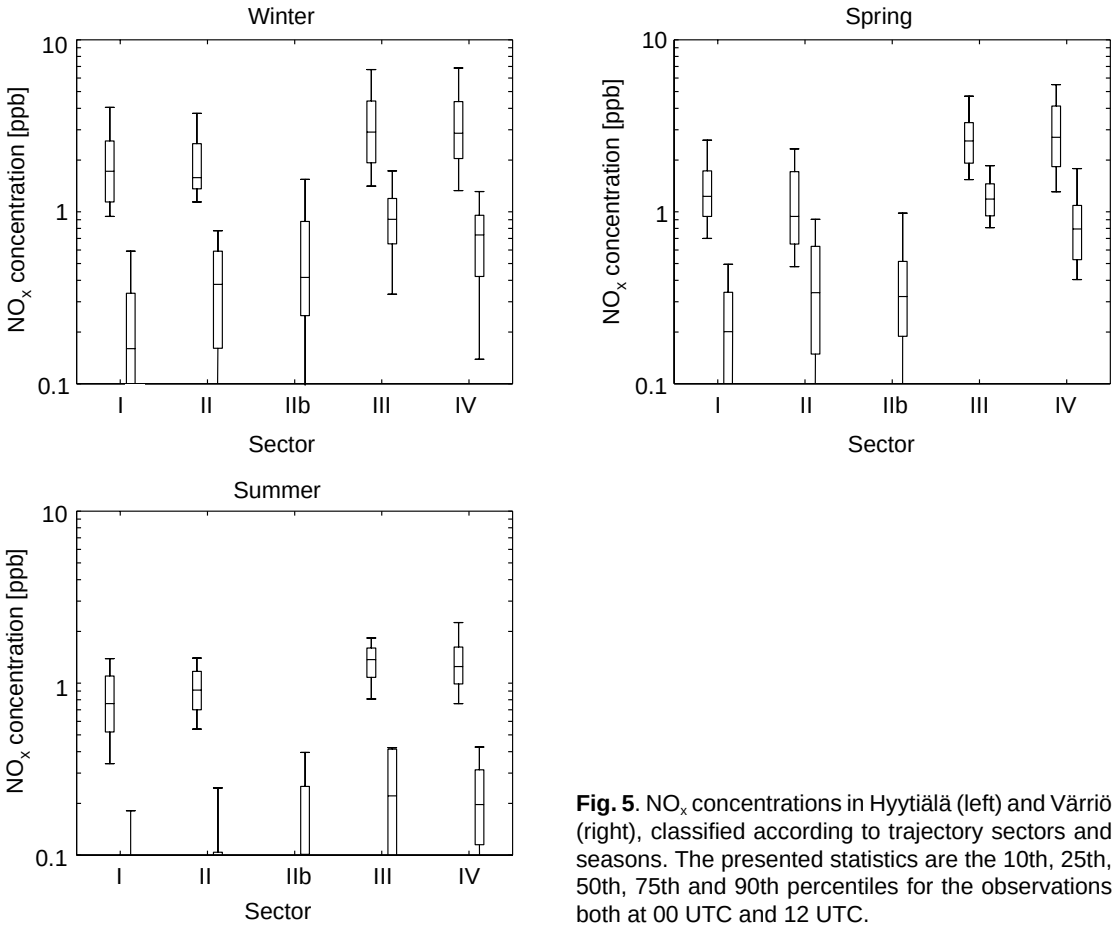

Fig. 5. NO_x concentrations in Hyytiälä (left) and Värriö (right), classified according to trajectory sectors and seasons. The presented statistics are the 10th, 25th, 50th, 75th and 90th percentiles for the observations both at 00 UTC and 12 UTC.

ured in summer, when in Värriö the concentrations were close to the detection limit (0.1 ppb). The seasonal cycle can partly be explained by differences in atmospheric mixing during the long-range transportation and partly by an increase in emissions from closely located sources during winter months (e.g. an increase in energy consumption due to heating). A clear southward NO_x gradient was observed when comparing the concentrations at two sites. This is in agreement with the observations in Norwegian Arctic (Solberg *et al.* 1997).

The highest NO_x concentrations were measured in air masses arriving at Hyytiälä and Värriö from more polluted continental Europe, i.e. from south-west Russia (III) and from Central Europe (IV). Then the measured concentrations were approximately twice as high as those from sectors I and II. This was a trend observed regardless of the season. Similar air mass dependence was observed in Norwegian Arctic in spring 1994 (Solberg *et al.* 1997). The concentrations in Hyytiälä were two to four times higher than the concentrations in Värriö because of the smaller distance to the industrial sources, especially in St. Petersburg's area southeast of Finland. The air from the Arctic Ocean brought especially low NO_x concentrations to Värriö.

No significant diurnal variation in NO_x concentration was found in Värriö. However, in Hyytiälä the daytime concentrations were slightly higher than the nighttime ones in winter, especially in cases when the air masses came from sectors I and IV.

Sulphur dioxide

The highest SO_2 concentrations were observed in winter at both the stations, and the lowest concentrations in summer (Fig. 6). This can be ex-

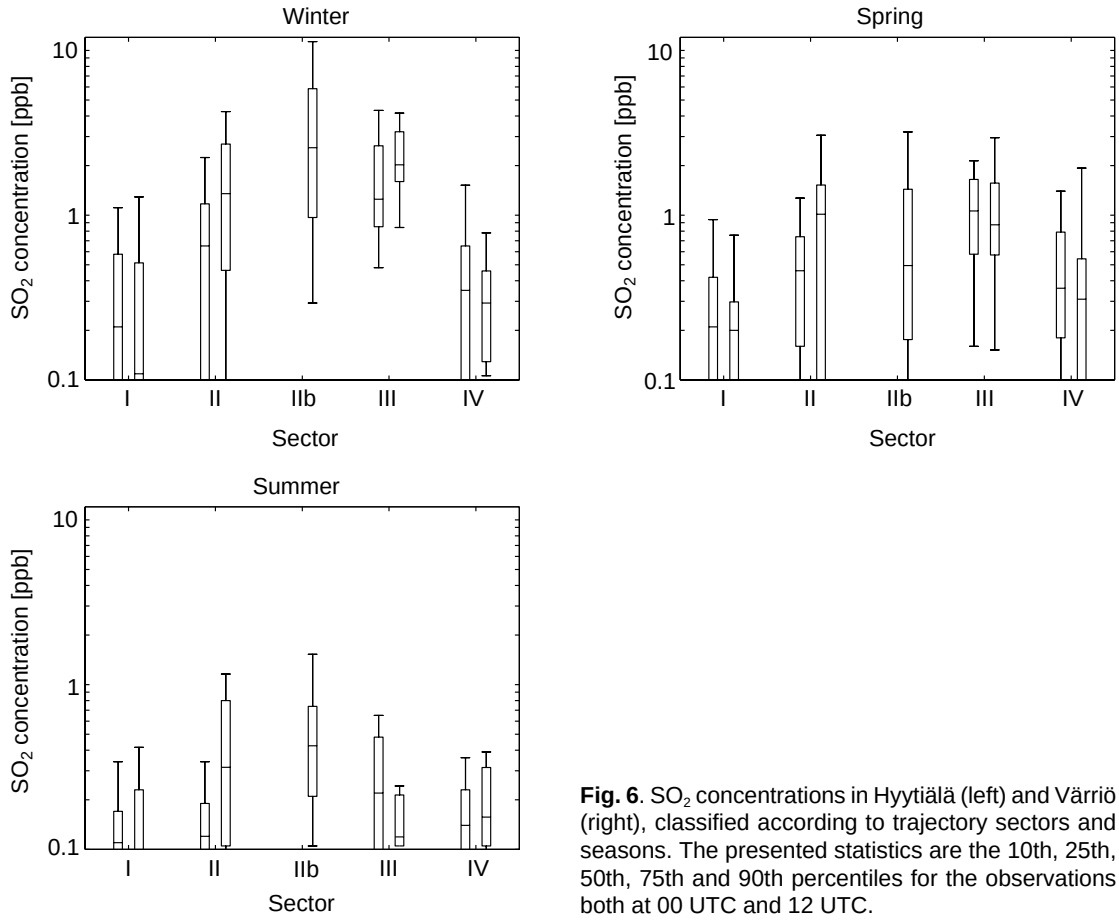

Fig. 6. SO_2 concentrations in Hyytiälä (left) and Värriö (right), classified according to trajectory sectors and seasons. The presented statistics are the 10th, 25th, 50th, 75th and 90th percentiles for the observations both at 00 UTC and 12 UTC.

plained by human activities (burning of fossil fuels) and an increased transport range due to the lack of photochemical transformation of SO_2 and less mixing with the higher atmosphere in winter.

The concentrations arriving from the Arctic Ocean (sector I) were very low at both measurement sites all over the year (Fig. 6). Also the concentrations from Central Europe (IV) were quite low. The highest concentrations in Hyytiälä were measured throughout the year in air masses coming from south-west Russia and the industrial district in St. Petersburg region (III). In Värriö, the highest concentrations were detected in air masses coming from Russia: from Kola Peninsula (IIb) in winter and summer, and from Russia (sectors II and III) in spring.

In Värriö, the concentrations from area II were much higher than in Hyytiälä. Some very high peaks were seen when air masses passed through the industrial area of Kola Peninsula (IIb) especially in winter (90th percentile value near 12 ppb). High peaks were also observed in spring and summer. No significant diurnal variation in SO_2 concentrations was found.

Water

Seasonal variation in water concentration shows that high values (median over all trajectory classes 11.8 g m^{-3}) were measured in summer and low values (median 4.2 g m^{-3}) in winter. In winter, and in spring air masses containing more water arrived mainly from sectors IV and I (Central Europe and the Arctic Ocean, Fig. 7), as expected. In summer, the highest water content of air came

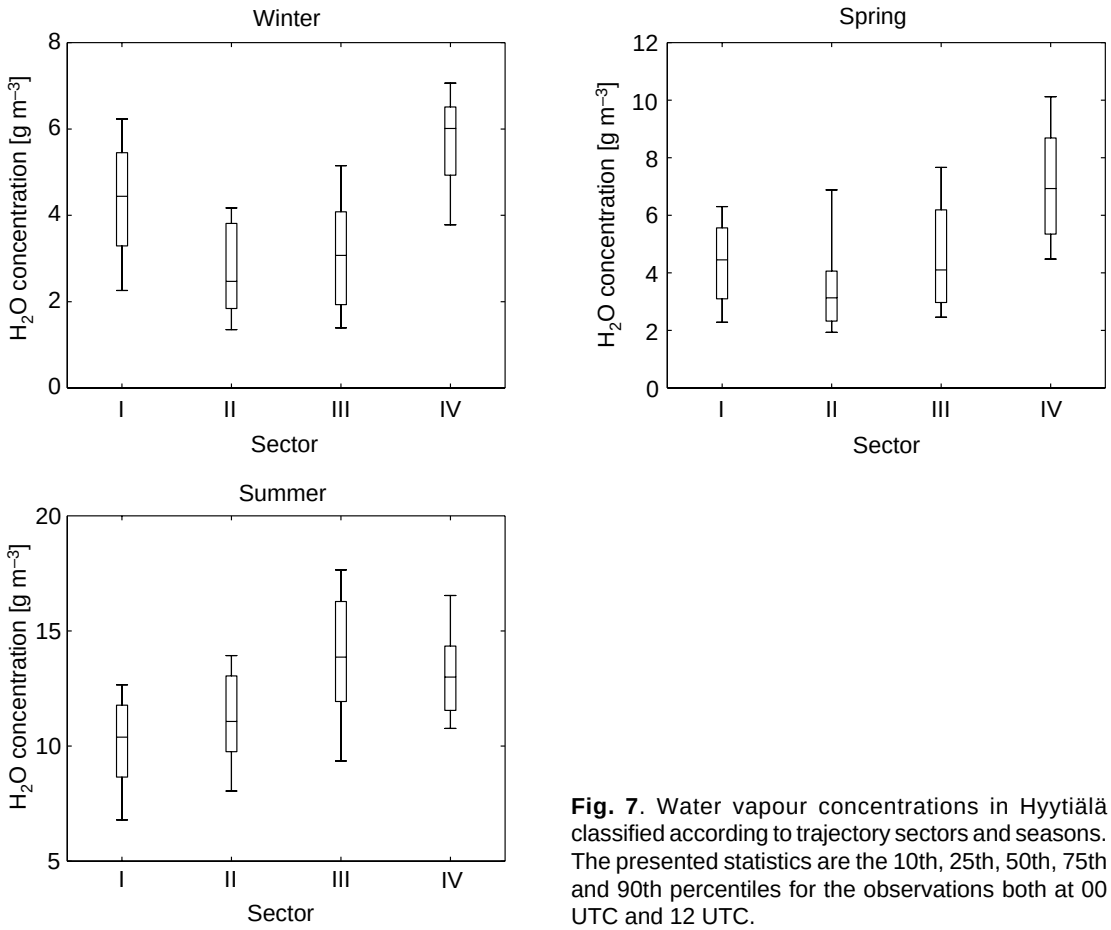

Fig. 7. Water vapour concentrations in Hyytiälä classified according to trajectory sectors and seasons. The presented statistics are the 10th, 25th, 50th, 75th and 90th percentiles for the observations both at 00 UTC and 12 UTC.

from sector III (south-west Russia), with water concentrations more than four times as high as wintertime concentrations from the same area. Furthermore, the lowest values were measured from sector I (the Arctic Ocean). No significant diurnal variation in air water content was observed.

Carbon dioxide

In winter and in spring, high CO_2 concentrations come to Hyytiälä from sectors III and IV (south-west Russia and Europe) (Fig. 8). This is a very common feature for pollution-related gases. CO_2 emissions to the atmosphere are due to burning of fossil fuels and biomass. In winter and spring, the median CO_2 concentration was about 369 ppm from sectors III and IV. The air masses from the other sectors brought approximately 364 ppm. In summer, the values were lower than in winter and in spring.

Also the forest-atmosphere CO_2 exchange is important for the concentrations in Hyytiälä. Generally the respiration of the ecosystem is higher in autumn because of the higher temperature, and depressed in winter when the temperature is lower. In autumn, the forest becomes a source of CO_2 to the atmosphere, and starts to act as a sink in spring, when daily photosynthesis exceeds respiration. Therefore, in summer the median of carbon dioxide concentration over all trajectories and arrival times was about 359 ppm and at other seasons it was about 366–367 ppm. For the same reason, the concentrations at night were higher than at day, except in winter when the values were almost the same. In summer, the median CO_2 con-

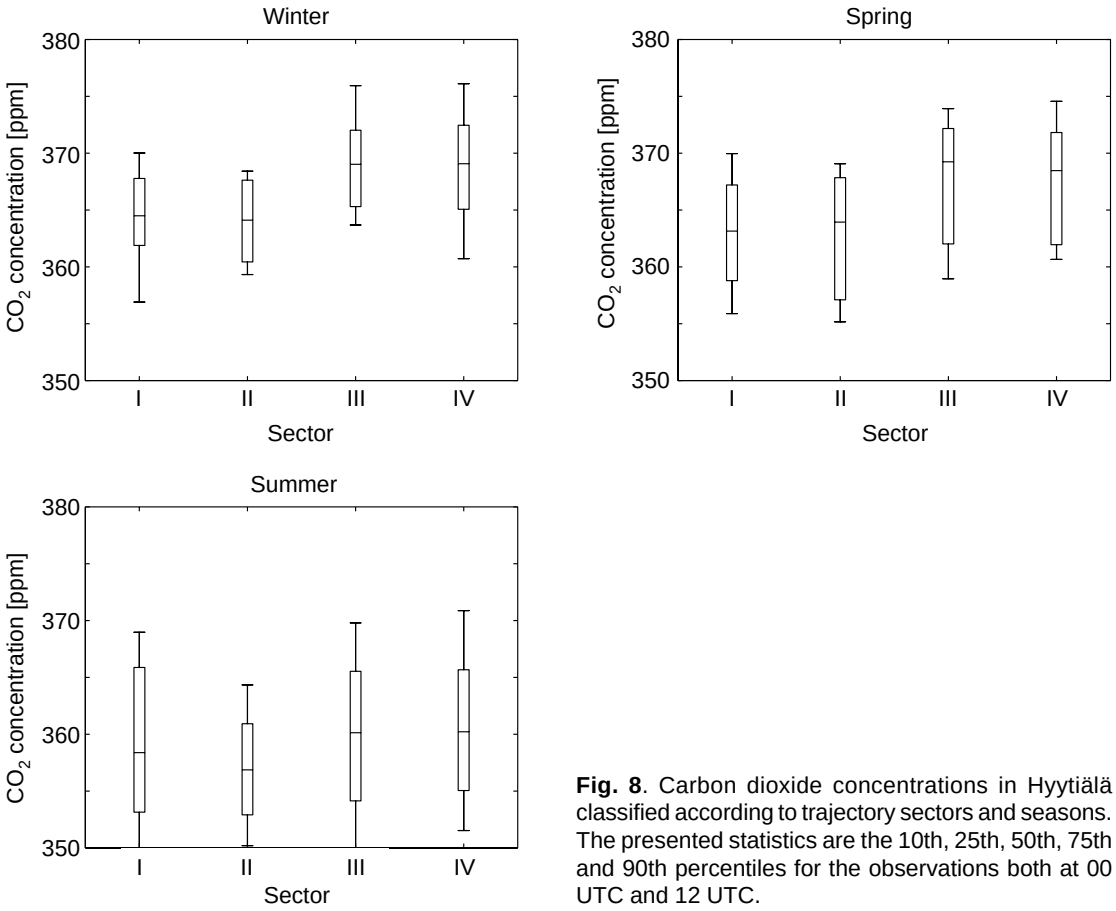

Fig. 8. Carbon dioxide concentrations in Hyytiälä classified according to trajectory sectors and seasons. The presented statistics are the 10th, 25th, 50th, 75th and 90th percentiles for the observations both at 00 UTC and 12 UTC.

centration was about 364 ppm at night and 355 ppm at day.

Aerosols

The aerosol concentrations in Värriö were typically smaller than in Hyytiälä (Fig. 9). The nighttime concentrations were somewhat smaller than daytime concentrations at both the sites. The wintertime concentrations were significantly smaller than the spring and summer concentrations. In spring, the highest concentrations occurred in air masses from sector I and were related to nucleation events. Beine *et al.* (1996) observed lowest aerosol particle concentrations in Arctic air masses during the spring of 1994 at Ny-Ålesund Zeppelin mountain station (78°55´N, 11°53´E, 474 m a.s.l). This might indicate the importance of biological factor in particle formation events.

Nucleation events are observed quite often in Hyytiälä and also in Värriö. Fig. 10 presents the fraction of trajectories accompanied with nucleation bursts for different sectors. Note that the low number of observed events can lead to unreliable results (particularly true in the winter plot). The highest fractions were observed in springtime for air masses coming from sectors I and II to Hyytiälä (almost 0.25) and to Värriö (around 0.1). In summer, the fractions were significantly smaller than in spring. In winter, no nucleation events were observed in Värriö.

The modal aerosol concentrations, obtained from the size spectrum measurements in Hyytiälä, were investigated. Modal structure of the aerosols was analysed by fitting two or three (depending on the concentration of smallest particles) log-

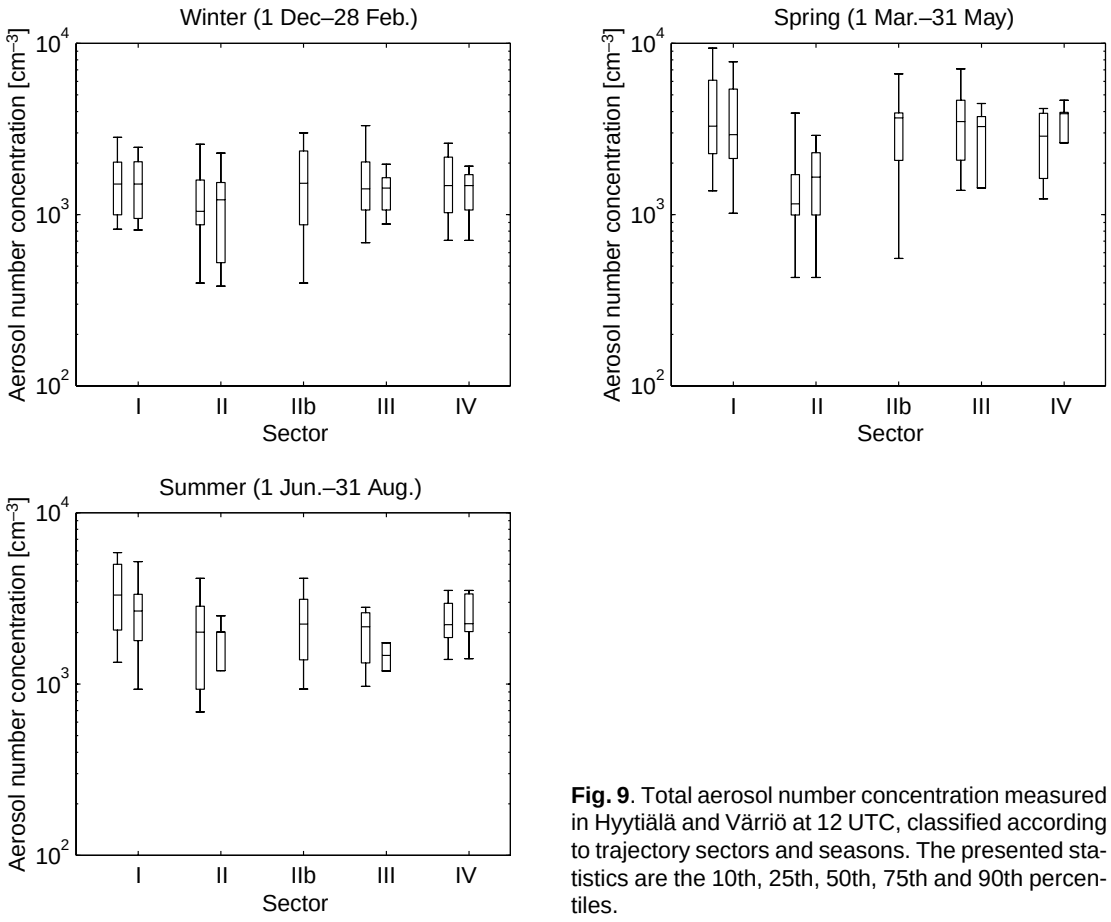

Fig. 9. Total aerosol number concentration measured in Hyytiälä and Värriö at 12 UTC, classified according to trajectory sectors and seasons. The presented statistics are the 10th, 25th, 50th, 75th and 90th percentiles.

normal modes to the measured particle size spectrum. From this data the concentration in each mode (nucleation, Aitken and accumulation modes) was calculated. The concentrations were calculated for each trajectory arrival time as an average over 40 minutes period.

The nucleation mode is defined as the smallest mode with a modal diameter less than 20 nm. The daytime nucleation mode had the highest concentration in spring (Fig. 11), particularly when the air was coming from the Arctic Ocean sector. The nighttime concentrations were always low.

The Aitken mode concentrations did not seem to vary much according to the sector of air origin (Fig. 11). The air masses from south-west Russia (III) and Central Europe (IV) sectors clearly dominated the accumulation mode concentrations, except in summer, when also sector II had quite high concentration values.

Chamber measurements

Gas exchange of pine shoots was measured during summers 1998 and 1999 in Hyytiälä and Värriö. The gas exchange measurements allowed us to study the net CO_2 exchange, the transpiration, the NO_x exchange, and the O_3 deposition on the shoot.

No significant variation of photosynthesis according to trajectory directions could be seen (Fig. 12). The main controlling environmental factor for photosynthesis is radiation. However, over two summers factors other than radiation affected the CO_2 exchange and the correspondence with radiation (*see* Fig. 3) could not be observed. The photosynthesis and transpiration in Hyytiälä were approximately twice as large as in Värriö (not shown). In Hyytiälä, the nighttime transpiration values were practically zero and the net CO_2-ex-

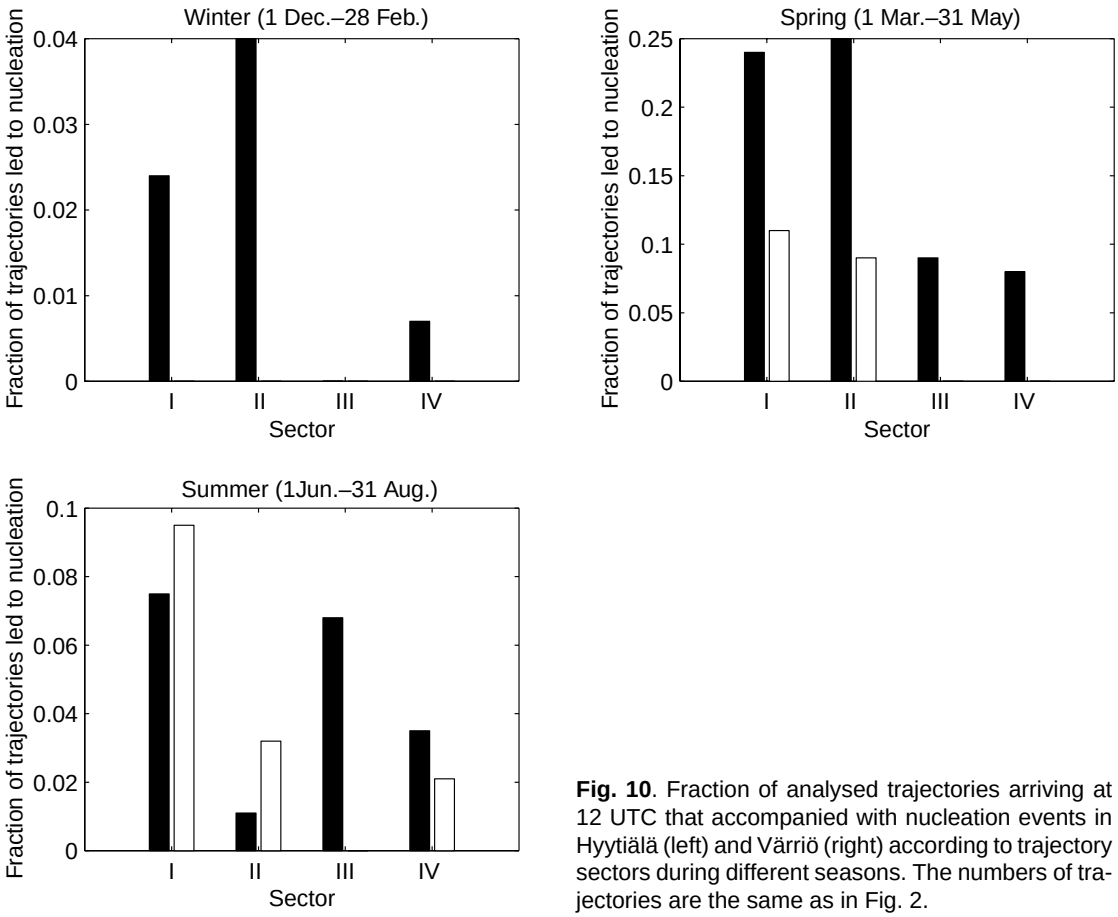

Fig. 10. Fraction of analysed trajectories arriving at 12 UTC that accompanied with nucleation events in Hyytiälä (left) and Värriö (right) according to trajectory sectors during different seasons. The numbers of trajectories are the same as in Fig. 2.

change was slightly negative, indicating respiration instead of photosynthesis. In Värriö, the nighttime values of photosynthesis and transpiration were often small but positive because of bright nights.

The ozone deposition was stronger when air arrived from sectors III and IV, when also the highest O_3 concentrations were observed. No connection between the O_3 deposition and radiation was observed. However, the NO_x emissions were largest for the Central Europe direction (sector IV), and the pattern of the NO_x emission statistics according to trajectory origin was similar to radiation. There was virtually no NO_x emission at night.

Fluxes

The turbulent fluxes of momentum, sensible heat, water vapour, carbon dioxide and aerosol particles, measured in Hyytiälä by the eddy covariance technique, were classified according to the trajectory origin.

The sensible heat fluxes behaved similarly to global radiation values shown in Fig. 3, as expected. As a feature in winter, the sensible heat fluxes within sector III air masses were predominantly upwards, while sensible heat was frequently transported also downwards during the other air masses. This is explained with the colder (relative to the surface) continental air arriving from sector III. The sensible heat fluxes at night were towards the surface and small compared to daytime values.

The absorption of momentum by the surface is determined by local characteristic, the aerodynamic roughness of the surface, and by the driving force, the large-scale air flow. The differences in momentum flux reflected the differences in prevailing synoptic situations, accompanying with

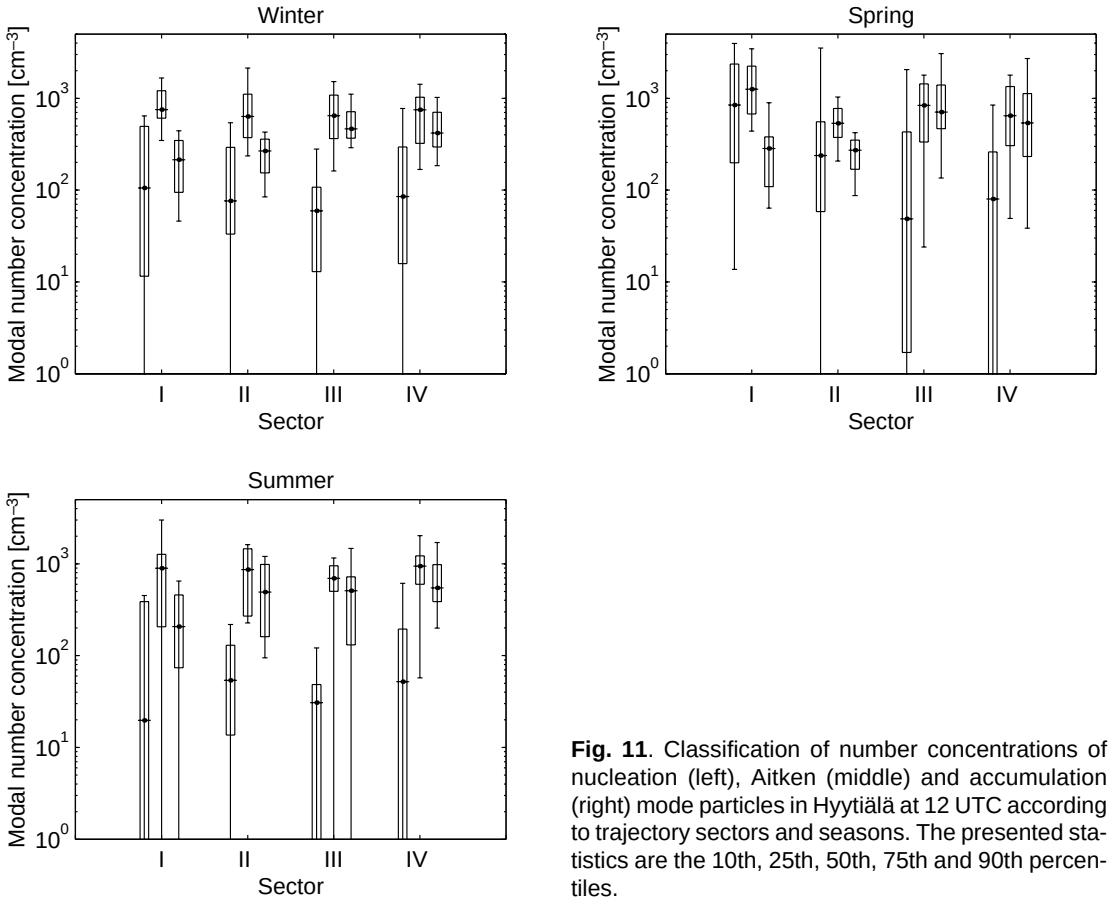

Fig. 11. Classification of number concentrations of nucleation (left), Aitken (middle) and accumulation (right) mode particles in Hyytiälä at 12 UTC according to trajectory sectors and seasons. The presented statistics are the 10th, 25th, 50th, 75th and 90th percentiles.

trajectory sectors. The momentum fluxes were significantly lower at night compared to daytime values during spring and summer seasons.

The water vapour flux was almost always upwards, and the rare negative values were close to zero. During the growing season, the main contribution to water flux comes from transpiration by trees, which is linked to their photosynthetic activity and ambient relative humidity. In winter, the water fluxes were small and rather well correlated with global radiation. The pattern was similar also for the spring and summer seasons.

In winter, the forest is a small source of CO_2 to the atmosphere. In spring, the highest CO_2 uptake occurred during northeast air origin. The high radiation corresponding to the Arctic Ocean trajectories (*see* Fig. 3) accompanied probably with low temperatures, and was not so favourable for photosynthesis. In summer, the CO_2 uptake was relatively even for all sectors, although there were significant differences in global radiation. This was similar to CO_2 exchange of shoots (Fig. 12).

The particle fluxes were available only for spring and summer seasons, from March to August. In the analysis the cases corresponding to local wind direction between 220 and 260 degrees were neglected as possibly affected by local pollution sources (the station buildings). Negative flux values correspond to the deposition of particles. The statistics have been obtained from limited number of cases for each sector: 20, 26, 20 and 38 together for spring and summer seasons for the sectors from I to IV, respectively. Sector I differs clearly from others: the trajectories arriving from the Arctic Ocean often brought nucleation events with them, and large downward particle fluxes were associated with the events (Fig. 13). For the spring period, only one observation of a large particle flux shifted the 10th percentile, corresponding to sector II trajectory, to a large

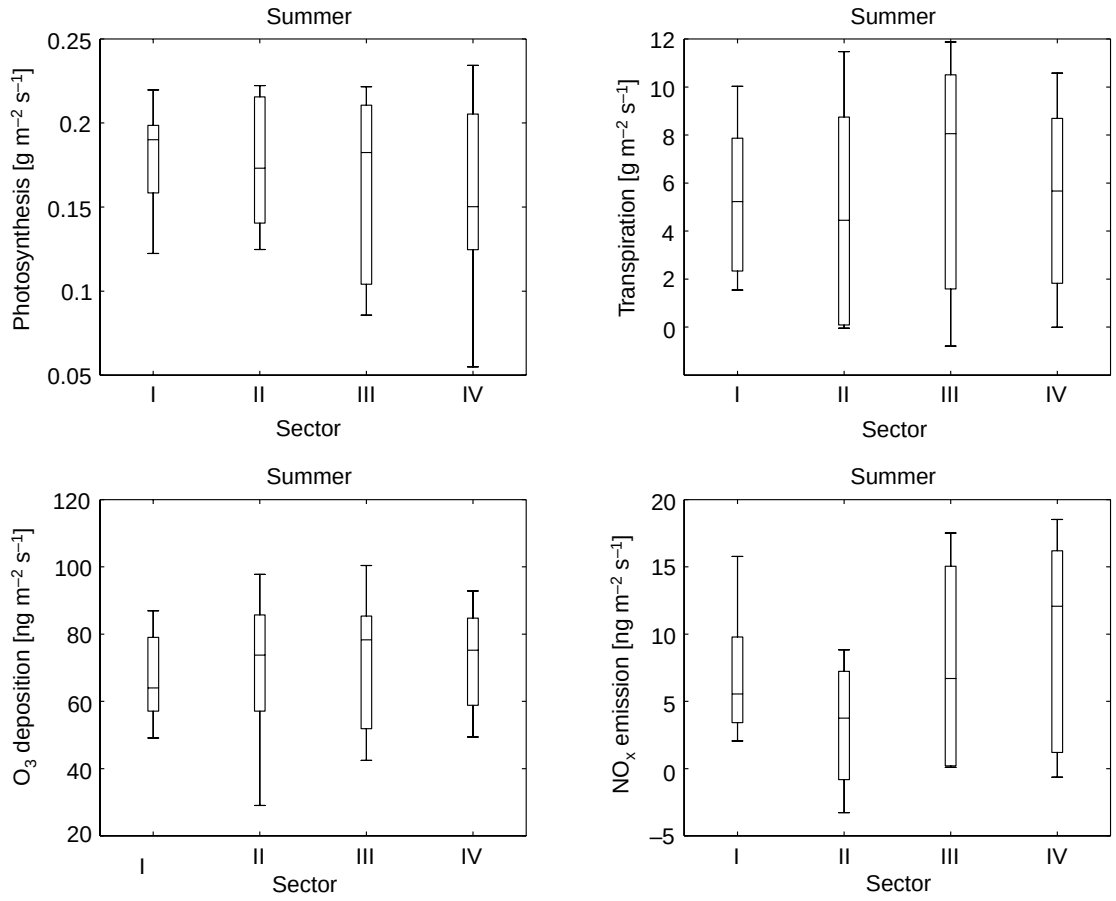

Fig. 12. Photosynthesis, transpiration, O_3 deposition and NO_x emission from/to pine shoot per unit needle area in Hyytiälä at 12 UTC during the summer season, classified according to trajectory origin. The presented statistics are the 10th, 25th, 50th, 75th and 90th percentiles.

negative value. In summer, the statistics corresponding to southeast trajectories (sector III) reflect presence of large negative fluxes, characteristic to nucleation events. These correspond however only to 7 cases, three of which were smaller than -5×10^6 m^{-2} s^{-1}.

Conclusions

In winter, the air masses from over the northeast and southeast Russia (sectors II and III; *see* Table 1 for sectors) brought lower temperatures, which was not the case in summer. In summer, the southern air masses were the warmest. The highest radiation fluxes in winter were observed during airflow from northeast (sector II), which corresponded in summer to lowest short wave radiation input in Hyytiälä, but not in Värriö. The highest radiation in summer was observed during the air masses from the Arctic Ocean. In spring the highest radiation corresponded to northern air origins (sectors I and II). The high radiation was related typically to low cloudiness arriving from these sectors. In these airflows also nucleation events occurred frequently. In spring and summer the relative humidity was higher in southwest airflow and lower in the air from the Arctic Ocean.

According to concentrations of tracers of air pollution in air masses, the sectors can be correspondingly divided into typically clean sectors (I and II) and polluted sectors (III and IV). Southwest Russia together with the industrial district of St. Petersburg is located in sector III and the polluted areas of Central Europe in sector IV.

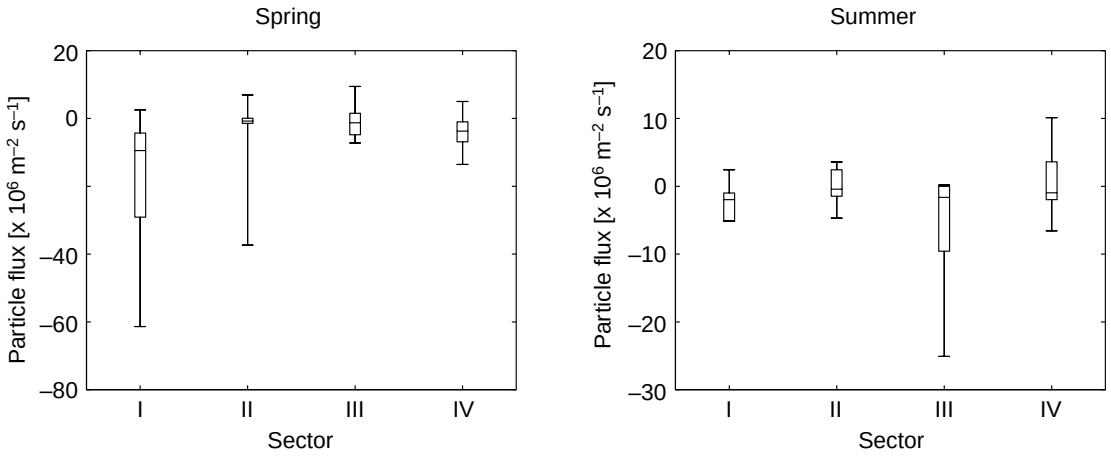

Fig. 13. Particle number fluxes measured in Hyytiälä at 12 UTC as classified according to air mass sectors and seasons. The presented statistics are the 10th, 25th, 50th, 75th and 90th percentiles.

What it comes to ozone concentrations, there was a clear difference between clean and polluted air masses. In wintertime the polluted air acts as a sink for ozone and in spring and summertime mainly as a source. Therefore, the air masses from sectors III and IV brought to both Hyytiälä and Värriö high O_3 concentrations in spring and summer, and low concentrations in winter. Consistently, also higher deposition of O_3 on pine shoots was observed in summer during the flow from sectors III and IV. Regardless of the season, these air masses contained the highest NO_x levels. The NO_x concentrations in flows from these sectors were almost twice as high as in flows from sectors I and II. The SO_2 concentrations in sector IV air masses were quite low. The highest SO_2 concentrations were measured in Hyytiälä in air masses from south-west Russia (III). In Värriö the highest SO_2 concentrations were detected in air masses arriving from Russia: from south-west Russia (III) in winter and in spring, but also from northern Russia and Kola Peninsula (II). In Värriö, the SO_2 concentrations from area II were much higher than in Hyytiälä, and some very high peaks were observed in winter when air masses passed through the industrial area of Kola Peninsula.

Some clear differences also in aerosol properties between clean and polluted air were observed. In polluted air masses accumulation mode concentrations were higher. The analysis of nucleation events showed that nucleation typically occurred in clean air masses. In spring, the nucleation occurred in about 25% of cases in Hyytiälä and about 10% of cases in Värriö when air mass originated from clean sectors. The frequency of nucleation events corresponding to polluted air sectors was much lower. During the nucleation events large downward aerosol particle number fluxes were measured.

Although there were some differences in air mass characteristics in Hyytiälä and Värriö, the overall behaviour was similar at both the sites.

References

Ahonen T., Aalto P., Rannik Ü., Kulmala M., Nilsson E.D., Palmroth S., Ylitalo H. & Hari P. 1997. Variations and vertical profiles of trace gas and aerosol concentrations and CO_2 exchange in eastern Lapland. *Atmos. Environ.* 31: 3351–3362.

Avila A. & Alarcon M. 1999. Relationship between precipitation chemistry and meteorological situations at a rural site in NE Spain. *Atmos. Environ.* 33: 1663–1677.

Beine H.J., Engardt M., Jaffe D.A., Hov Ø., Holmen K., & Stordal F. 1996. Measurements of NOx and aerosol particles at the Ny-Ålesund Zeppelin mountain station on Svalbard: Influence of regional and local pollution sources. *Atmos. Environ.* 30: 1067–1079.

Finlayson-Pitts B.J. & Pitts J.N. 2000. *Chemistry of the Upper and Lower Atmosphere.* Academic Press.

Hari P., Kulmala M., Pohja T., Lahti T., Siivola E., Palva L., Aalto P., Hämeri K., Vesala T., Luoma S. & Pulliainen E. 1994. Air pollution in eastern Lapland: challenge for an environmental measurement station. *Silva Fennica* 28(1): 29–39.

Hjellbrekke A.-G. 1999. *Ozone measurements 1997.* EMEP/CCC-Report 2/99. Norwegian Institute for Air Research, Kjeller, Norway.

Holton J.R. 1992. *An introduction to dynamic meteorology*. Academic Press, San Diego, California.

Houghton J.T., Meira Filho L.G., Callander B.A., Harris N., Kattenburg A. & Maskell K. (eds.) 1996. *Climate Change 1995*. IPCC, Cambridge University Press, Cambridge.

Kahl J.D., Harris J.M., & Herbert G.A. 1989. Intercomparison of three long-range trajectory models applied to Arctic Haze. *Tellus* 41B: 524–536.

Kleinman L. 1991. Seasonal dependence of boundary layer peroxide concentration: The low and high NOx regimes. *J. Geophys. Res.* 96: 20721–20733.

Kulmala M., Toivonen A., Mäkelä J.M. & Laaksonen A. 1998. Analysis of the growth of nucleation mode particles observed in Boreal forest. *Tellus* 50B: 449–462.

Kulmala M., Mäkelä J.M., Hämeri K., Aalto P.P, Pirjola L., Väkevä M., Koponen I.K., Buzorius G., Keronen P., Rannik Ü., Seidl W., Forkel R., Hoffmann T., Spanke J., Nilsson E.D., Jansson R., Hansson H.-C., O'Dowd C., Becker E., Paatero J., Hillamo R., & Viisanen Y. Biogenic aerosol formation in the boreal forest. ***Boreal Env. Res.* 5: XX–XX**.

Laurila T. 1999. Observational study of transport and photochemical formation of ozone over northern Europe. *J. Geophys. Res*. 104: 26235–26243.

Lopez A., Fontan J. & Minga A. 1993. Analysis of atmospheric ozone measurements over a pine forest. *Atmos. Environ.* 27A: 555–563.

Mäkelä J.M., Aalto P., Jokinen V., Nissinen A., Palmroth S., Markkanen T., Seitsonen K., Lihavainen H. & Kulmala M. 1997. Observations of ultrafine aerosol particle formation in boreal forest. *Geophys. Res. Lett*. 24: 1219–1222.

Mäkelä J.M., Dal Maso M., Pirjola L., Keronen P., Laakso L. & Kulmala M. 2000. Characteristics of the aerosol particle formation events observed at a boreal forest site in southern Finland. ***Boreal Env. Res.* 5: XX–XX**.

Pirjola L., Laaksonen A., Aalto P. & Kulmala M. 1998. Sulfate aerosol formation in the Arctic boundary layer. *J. Geophys. Res*. 103: 8309–8322.

Pöllänen R., Valkama I. & Toivonen H. 1997. Transport of radioactive particles from the Chernobyl accident. *Atmos. Environ*. 31: 3575–3590.

Rummukainen M., Laurila T., & Kivi R. 1996. Yearly cycle of tropospheric ozone at the Arctic circle. *Atmos. Environ.* 30: 1875–1885.

Scheel H.E., Areskoug H., Geiß H., Gomiscek B., Granby K., Haszpra L., Klasinc L., Kley D., Laurila T., Lindskog A., Roemer M., Schmitt R., Simmonds P., Solberg S. & Toupange G. 1997. On the spatial distribution and seasonal variation of lower-troposphere ozone over Europe. *J. Atmos. Chem.* 28: 11–28.

Seinfeld J.H. & Pandis S.P. 1998. *Atmospheric chemistry and physics*. John Wiley & Sons.

Simmonds P.G., Seuring S., Nickless G. & Derwent R.G. 1997. Segregation and interpretation of ozone and carbon monoxide measurements by air mass origin at the TOR station Mace Head, Ireland from 1987 to 1995. *J. Atmos. Chem.* 28: 45–59.

Solberg S., Krognes T., Stordal F., Hov Ø., Beine H.J., Jaffe D.A., Clemitshaw K.C. & Penkett S.A. 1997. Reactive nitrogen compounds at Spitsbergen in the Norwegian Arctic. *J. Atmos. Chem.* 28: 209–225.

Stohl A. 1998. Computation, accuracy and applications of trajectories — a review and bibliography. *Atmos. Environ.* 32: 947–966.

Stohl A. 1996. Trajectory statistics — A new method to establish source-receptor relationships of air pollutants and its application to the transport of particulate sulphate in Europe. *Atmos. Environ.* 30: 579–587.

Tammelin B. 1991. *Finnish wind atlas*. Finnish Meteorological Institute, Helsinki.

Tarrasón L., Semb A., Hjellbrekke A.-G., Tsyro S., Schaug J., Bartnicki J. & Solberg S. 1998. *Geographical distribution of sulphur and nitrogen compounds in Europe derived both from modelled and observed concentrations*. EMEP/MSC-W Note 4/98. Norwegian Meteorological Institute, Oslo and Norwegian Institute for Air Research, Kjeller, Norway.

Valkama I. & Pöllänen R. 1996. Transport of radioactive materials in convective clouds. In: Kulmala M. & Wagner P.E. (eds.), *Nucleation and atmospheric aerosols 1996,* Elsevier Science Ltd, Oxford, England, pp. 411–414.

Vesala T., Haataja J, Aalto P., Altimir N., Buzorius G., Garam E., Hämeri K., Ilvesniemi H., Jokinen V., Keronen P., Lahti T., Markkanen T., Mäkelä J.M., Nikinmaa E., Palmroth S., Palva L., Pohja T., Pumpanen J., Rannik U., Siivola Y., Ylitalo H., Hari P. & Kulmala M. 1998. Long-term field measurements of atmosphere-surface interactions in boreal forest combining forest ecology, micrometeorology, aerosol physics and atmospheric chemistry. *Trends in Heat, Mass & Momentum Transfer* 4: 17–35.

Virkkula A., Mäkinen M., Hillamo R. & Stohl A. 1995. Atmospheric aerosol in the Finnish Arctic: particle number concentrations, chemical characteristics, and source analysis. *Water, Air and Soil Pollution* 85: 1997–2002.

Virkkula A., Hillamo R.E., Kerminen V.-M. & Stohl A. 1997. The influence of Kola Peninsula, continental European and marine sources on the number concentrations and scattering coeffcients of the atmospheric aerosol in Finnish Lappland. *Boreal Env. Res.* 2: 317–336.

Wotawa G. & Kröger G. 1999. Testing the ability of trajectory statistics to reproduce emission inventories of air pollutants in cases of negligible measurement and transport errors. *Atmos. Environ.* 33: 3037–3043.

Received 24 March 2000, accepted 24 August 2000